

## Article

# Optimizing V2X Communication: Spectrum Resource Allocation and Power Control Strategies for Next-Generation Wireless Technologies

Ali. M. A. Ibrahim <sup>1</sup>, Zhigang Chen <sup>1,\*</sup>, Yijie Wang <sup>2</sup>, Hala A. Eljailany <sup>3</sup> and Aridegbe A. Ipaye <sup>1</sup>

<sup>1</sup> School of Computer Science and Engineering, Central South University, Changsha 410083, China; alimaher\_912@hotmail.com or alimahir@csu.edu.cn (A.M.A.I.); aa.ipaye@hotmail.com (A.A.I.)

<sup>2</sup> Institute of Big Data, Central South University, Changsha 410083, China; wangyijiecs@csu.edu.cn

<sup>3</sup> School of Traffic and Transportation Engineering, Central South University, Changsha 410000, China; halaej@csu.edu.cn

\* Correspondence: czg@csu.edu.cn

**Abstract:** The upcoming wireless technology developments in the next generations are expected to substantially transform the vehicle-to-everything (V2X) communication network. The challenge of limited spectrum resources in V2X communication, caused by the need for high data rates, necessitates a thorough analysis of spectrum resource allocation and power control. This complex problem falls under the domain of mixed-integer nonlinear programming; a strategic approach is implemented to overcome these issues, which divides the main challenge into two sub-problems. The issue of resource allocation is addressed by implementing a multiaccess spectrum allocation method, which is deliberately designed to optimize the utilization of the spectrum resources that are currently accessible. Concurrently, the power control issue is resolved by employing a continuous convex approximation technique, which effectively converts non-convex power-allocation issues into convex equivalents. This approach helps to alleviate interference between users. Finally, the simulation results prove that the proposed approaches can improve vehicle performance. The algorithms proposed in this article significantly improve the system throughput and access rate of vehicular user equipment (VUEs) while ensuring the data rate of cellular user equipment (CUEs).



**Citation:** Ibrahim, A.M.A.; Chen, Z.; Wang, Y.; Eljailany, H.A.; A. Ipaye, A. Optimizing V2X Communication: Spectrum Resource Allocation and Power Control Strategies for Next-Generation Wireless Technologies. *Appl. Sci.* **2024**, *14*, 531. <https://doi.org/10.3390/app14020531>

Academic Editors: Cheol-Ho Hong, Kyungwoon Lee and Youngpil Kim

Received: 2 December 2023

Revised: 29 December 2023

Accepted: 2 January 2024

Published: 8 January 2024



**Copyright:** © 2024 by the authors. Licensee MDPI, Basel, Switzerland. This article is an open access article distributed under the terms and conditions of the Creative Commons Attribution (CC BY) license (<https://creativecommons.org/licenses/by/4.0/>).

## 1. Introduction

In recent years, the evolution of wireless communication systems has propelled us into a transformative era of interconnected vehicles, marking a significant stride toward the realization of a more advanced vehicular landscape. These systems are poised to revolutionize vehicle-to-everything (V2X) communication networks [1,2]. The imperative for direct data exchange between vehicles has led to the incorporation of V2X in long-term evolution (LTE) and its enhancement in the 5G new radio (NR) standards [3–5]. The incorporation of these standards signifies a strategic move towards leveraging the advancements in wireless technologies to meet the dynamic communication requirements of interconnected vehicles [6,7]. In paving the way for connected vehicles, the forthcoming sixth generation (6G) is poised to adhere to more rigorous regulations governing vehicle connectivity, with features such as V2X low latency (0.001 s), robust connections, cutting-edge throughput for handling extensive data, and full automation collectively contributing to elevating its reliability [8,9]. The ongoing evolution of wireless communication, sensing, and computing technologies is instrumental in the deployment of intelligent transportation systems, with the overarching goal of making transportation more efficient and intelligent [10,11]. One significant stimulus for this progress is the implementation of V2X communication [12], which plays a vital

role in enhancing road safety, optimizing traffic efficiency, and facilitating the provision of information services [13,14]. The V2X communication network is designed to accommodate various applications, each with its specifications. It includes vehicle-to-infrastructure (V2I) communication, vehicle-to-vehicle (V2V) communication, and vehicle-to-pedestrian (V2P) communication [15–17]. However, the transition to 6G communications introduces a formidable challenge to the resource-allocation system, particularly when autonomous distributed vehicles are in operation, given the stringent requirements for extremely high throughput, low latency, and unwavering dependability [18,19]. This necessitates a comprehensive reassessment of the resource-management strategies to ensure the seamless integration of these cutting-edge technologies into the future landscape of connected and autonomous vehicles [20,21].

The primary objective of vehicular networks is to facilitate cooperative automated driving, thereby minimizing accidents and optimizing the efficient use of existing roadways [22,23]. However, achieving this goal poses significant challenges in terms of resource management and power control [24–26]. In the implementation of V2X communication, the critical issue of resource allocation naturally comes to the forefront, prompting researchers to devote considerable attention to the intricacies of V2X resource allocation [27,28]. One possible solution to the resource-allocation problem is to use device-to-device (D2D) technology, which supports direct communication between devices and can reuse the spectrum resources of cellular users, with many advantages such as low latency and high spectral efficiency [29]. Consequently, its application in V2X communication has evolved into an indispensable scenario in the next-generation mobile communication system [30,31]. The challenge of resource allocation in V2X communication stems from the reliance on conventional D2D technology. However, the unique attributes of vehicle communication, notably its capability for high-speed mobility, render resource-allocation methodologies tailored for D2D technology unsuitable for direct implementation in V2X communication [32]. Therefore, in light of the constraints posed by limited spectrum resources, the paramount objective is to devise an appropriate strategy for resource management that can effectively cater to the rigorous demands of V2X communication, particularly in meeting high-speed requirements.

### 1.1. Related Works

In recent studies, researchers have focused on optimizing network utilization by implementing base station power regulation in V2X communications. Ref. [33] introduced an algorithm to optimize resource allocation and maximize the potential for vehicle association with the base station (BS). The proposed approach employed adaptive adjustment of BS power to address the maximization problem, encompassing the Doppler effect and power selection considerations.

In [34], the authors examined the mathematical problem through power control techniques while considering the limitation of a restricted number of accessible resource blocks (RBs). The researchers' primary objective was to utilize a Lagrangian approach to address the problem through power allocation and resource block assignment. The authors [35] devised a methodology for addressing a Stackelberg game scenario by implementing power control techniques. The Stackelberg game was utilized in this study to examine the interaction between the BS and the user equipment (UE). The Stackelberg model was also investigated to obtain an ideal solution. The authors of [36] presented an ergodic search algorithm that is near-optimal in addressing the issue of power efficiency. This method aims to manage and regulate power consumption at the BS effectively. However, in the methods mentioned earlier, satisfying the minimal SINR requirements would only provide best-effort services to VUEs. As a result, these methods did not adopt the probability form required to ensure the need for ultra-reliable transmission. The outage probability of the SINR criteria for guaranteeing the VUE QoS (quality of service) must be lower than the default likelihood.

In [37], an algebraic constraint was developed to simplify the reliability requirements for VUEs represented as the tolerable VUEs chance constraints, and an analytical mapping approach was developed to determine the optimum transmit power for V2X networks. To handle the spectrum sharing problem in RIS-aided vehicular networks where the outage probability of V2V links is used to assure the dependability of V2V communication, the authors in [38] devised the block coordinate descent approach. V2V's minimal dependability criterion was ensured using chance constraints in [39], which also offered a suite of graph-based resource management algorithms to handle the resource-allocation problem. In [40], they addressed the issue of joint spectrum and power-allocation problems for V2X communication in the presence of imperfect channel state information (CSI). Bernstein approximations are utilized to convert the chance constraint into a computable constraint. A bisection search method is proposed to obtain the optimal allocation solution with reduced complexity efficiently.

There are currently different spectrum resource matching techniques between VUEs and CUEs in applying D2D technology to V2X communication. Authors in [41] proposed a new power-allocation method for energy efficiency optimization in D2D-based cellular V2X communication networks. In [42], they studied subcarrier allocation and power control problems to maximize the total data rate of V2I communication users under the reliability constraints of V2V communication users. In [43] the joint power control and resource-allocation problem of V2X communication when CSI is incomplete. The authors proposed a distributed robust power control algorithm while ensuring the reliability of cellular links [44].

### 1.2. Contribution

In the aforementioned resource distribution methods, the limited utilization of spectrum resources results in constrained throughput and restricted accessibility for VUEs. In multiaccess resource allocation, a pair of VUEs can utilize various subcarriers. At the same time, a single subcarrier can also be shared among numerous pairs of VUEs. This has the potential to enhance the efficiency of VUEs by increasing throughput and access rate while maximizing the utilization of spectrum resources. The main contributions of this article are as follows:

- We propose a multiaccess resource-allocation scheme for V2X communication that allows multiple VUEs to share the same subcarrier and one pair of VUEs to use multiple subcarriers, which can improve the spectrum utilization and data rate of V2X communication.
- We design a three-stage algorithm to solve the subcarrier-allocation problem for CUEs and VUEs. The algorithm first allocates subcarriers to CUEs to ensure their data rate requirements, then allocates the remaining subcarriers to VUEs, and finally allows VUEs to reuse the subcarriers already allocated to other users.
- We formulate the power control problem as a mixed integer nonlinear programming problem and solve it using the successive convex approximation method, which can transform the non-convex problem into a convex problem and obtain the optimal power-allocation solution.
- To ensure the effectiveness of the proposed method and algorithms, we have simulated them in MATLAB. Regarding the access rate and throughput for VUEs, the paper evaluates the suggested approach against the current literature. The research also investigates the impact of numerous characteristics on the system performance, such as the number of VUEs, the number of CUEs, and the vehicle speed. The study demonstrates that the suggested method can effectively raise the bar for both access rate and throughput for VUEs while still meeting the needs of the CUEs in terms of required data rates.

Hence, this paper employs a multiaccess resource-allocation strategy and joint power control to optimize the system throughput of VUEs while simultaneously guaranteeing the data rate of CUEs. The implementation of multiaccess matching algorithms has the poten-

tial to enhance system performance by employing effective power control and resource-allocation techniques. Nevertheless, this technique gives rise to significant co-channel interference on cellular and vehicle networks. Hence, the challenge addressed in this article is the rational allocation of spectrum resources and mitigating interference.

The rest of the paper is organized as follows. Section 2 describes the system model and the problem description. The proposed multiaccess resource allocation and power control algorithms are included in Section 3. In Section 4, simulation results and analysis are reported. Section 5 concludes the paper.

## 2. System Model and Problem Formulation

In V2X communication, resource allocation and power control are crucial. As we study our system model, we focus on the dynamic interaction between vehicles and infrastructure. We aim to understand V2X resource allocation and power control optimization through a detailed problem formulation.

### 2.1. System Model

The paper presents a system model, as depicted in Figure 1, which focuses on a multi-user OFDMA V2X communication network with a single BS, which is a technique that allows multiple users to access the same channel by dividing it into smaller subchannels or subcarriers. Each subcarrier can be assigned to a different user, depending on their channel conditions and data rate requirements [45]. This way, the spectrum resources can be utilized more efficiently, and the interference can be reduced. In contrast to conventional device-to-device users, individuals utilizing vehicles exhibit a higher movement velocity. Variations in vehicle speed and safety distance exist to prioritize safety, leading to distinct location modeling approaches for vehicle users compared to D2D users. On average, highway models [46,47] show a spacing of 2.5 m between cars. Assuming that traffic is moving in a straight line at a constant speed, the distribution of car positions on the road can be described by a Poisson process. Y vehicles need V2I communication, denoted as CUEs, and X pairs of vehicles need V2V data transmission, denoted as VUEs (where  $X > Y$ ). The quantity of subcarriers is denoted as  $V$ . To meet the data rate demands of CUEs, the subcarriers are orthogonally allocated to the CUEs, so there is no interference between the CUEs. To enhance spectrum utilization and VUEs' data rate, each pair of VUEs can use multiple subcarriers, and to allow more VUEs to access, each subcarrier also allows multiple VUEs to use it, that is, a multiaccess resource match scheme. The allocation of uplink subcarriers has been regarded as a potential solution to the co-channel interference problem of uplink resources, which is more effectively addressed than the downlink.

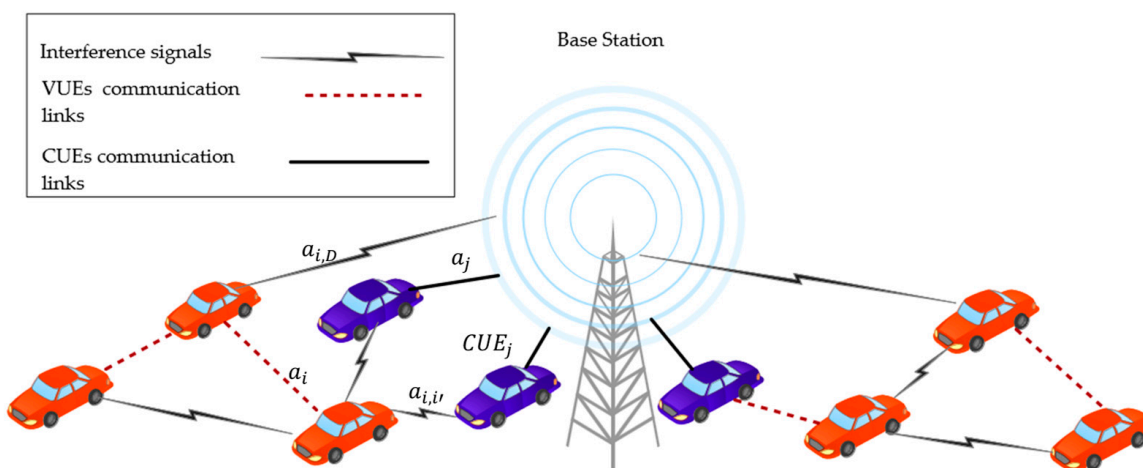


**Figure 1.** System model.

## 2.2. Problem Description

Assuming all links are independent block fading channels, CSI can be approximately constant in each time interval. At the beginning of each time interval, CUEs use uplink resources to report the cellular link CSI to the BS. For the VUEs, during the V2V discovery phase, the receiving end of VUEs reports the CSI of the vehicle link to the BS using uplink resources. However, due to the Doppler effect brought about by the high mobility of vehicles, the vehicle link will undergo rapid changes in small-scale fading. In this case, if CSI is continuously updated to the BS, it will result in high signaling overhead [48]. Therefore, the system model in this article only considers large-scale fading to reduce the network overhead. In addition, this article assumes that the vehicle speeds are all the same, so the Doppler effect between vehicles can be ignored. We define VUE $i$  as the  $i$ -th VUE; similarly, CUE $j$  is the  $j$ -th CUE.

We define  $a_{j,i}^v$  as the channel power gain of the interference link between the transmitting end of CUE $j$  and the receiving end of VUE $i$  on the  $v$ -th subcarrier, represented as

$$a_{j,i}^v = A\delta_{j,i}dis_{j,i}^{-\omega}, \quad (1)$$

In the equation,  $A$  is the path loss constant, with  $\delta_{j,i}$  representing the shadow fading between VUE $i$  and CUE $j$ . This shadow fading follows a lognormal distribution. The parameter  $dis_{j,i}$  is the distance between the receiving end of VUE $i$  and the transmitting end of CUE $j$ , and  $\omega$  is the path loss index. Additionally,  $a_j^v$  is defined as the communication link channel power gain from CUE $j$  to the BS,  $a_i^v$  is the channel power gain of the communication link of VUE $i$ ,  $a_{i,D}^v$  is the interference channel power gain from VUE $i$  sharing subcarrier  $v$  to the BS, and  $a_{i',i}^k$  is the interference channel power gain between the transmitting end of VUE $i'$  and the receiving end of VUE $i$  sharing subcarrier  $v$ .

The signal-to-interference plus noise ratio (SINR) of VUE $i$  is represented as

$$\psi_i^v = \frac{W_i^v a_i^v}{\theta^2 + \sum_{i'=i}^X C_{i'}^v W_{i'}^v a_{i',i}^v + \sum_j^Y C_j^v W_j^v a_{j,i}^v}, \quad (2)$$

$W_j^v$  represents the transmission power of VUE $i$  on the  $v$ -th subcarrier.  $C_{i'}^v$  represents the binary variable that represents the mapping relationship between the subcarrier  $v$  and VUE $i'$ . If VUE $i'$  allows the use of the subcarrier  $v$ , then  $C_{i'}^v = 1$ ; otherwise  $C_{i'}^v = 0$ .  $\theta^2$  is the variance of zero mean Gaussian noise. Since a subcarrier is allowed to be used by multiple VUEs, therefore, interference to VUE $i$  includes other VUEs and CUE using the subcarrier  $v$ .

The SINR of CUE $j$  is represented as

$$\psi_j^v = \frac{W_j^v a_j^v}{\theta^2 + \sum_i^X C_i^v W_i^v a_{i,D}^v}, \quad (3)$$

In the formula, we represent the SINR of CUE $j$  when using the  $v$ -th subcarrier, where  $W_j^v$  represents the transmission power of CUE $j$  on the  $v$ -th subcarrier. Due to the orthogonal spectral resources between CUEs, the interference to CUEs is only caused by VUEs that jointly use the subcarrier  $v$ .

## 2.3. Optimization Model

The objective of this article is to optimize the aggregate data rate of VUEs by integrating subcarrier allocation and power control techniques for both CUEs and VUEs, while simultaneously guaranteeing the minimum data rate requirements of all CUEs. This study examines a multiaccess resource matching strategy as a means to enhance the system throughput of VUEs. The optimization problem is formulated as a mixed-integer nonlinear programming (MINP) problem, which is generally difficult to solve. Therefore, the problem is divided into two subproblems: the resource-allocation problem and the power control problem. The resource-allocation problem determines the binary variables

$C_i^v$  and  $C_j^v$  using a heuristic algorithm that assigns subcarriers to CUEs and VUEs in a multiaccess manner. The power control problem determines the continuous variables using a successive convex approximation (SCA) method that transforms the non-convex problem into a convex problem.

The optimization problem formulation is presented as follows.

$$\begin{aligned}
 \text{Problem 1 :} \quad & \max_{\{C_i^v, C_j^v, W_i^v\}} \sum_{i=1}^X \sum_{v=1}^V (\log(1+\psi_i^v)), \\
 \text{s.t.} \\
 c1 : \quad & C_i^v, C_j^v \in \{0, 1\}, \forall v \in V, \forall j \in Y, \forall i \in X, \\
 c2 : \quad & \sum_j^Y C_j^v \leq 1, \forall v \in V, \\
 c3 : \quad & W_i^v \leq W_i^{max}, \forall i \in X, \\
 c4 : \quad & W_j^v \leq W_j^{max}, \forall j \in Y, \\
 c5 : \quad & \sum_{v=1}^V \Psi_j^v \geq \Psi_j^{size}, \forall j \in Y
 \end{aligned} \tag{4}$$

Equation (4) is the objective function and the constraints for maximizing the sum of the data rates of the VUEs. Here are the parameters in Equation (4):  $C_i^v$  and  $C_j^v$  are the binary variables that indicate the mapping relationship between subcarrier  $v$  and VUEi or CUEj. If VUEi or CUEj is allowed to use the subcarrier  $v$ , then  $C_i^v$  or  $C_j^v$  is 1; otherwise it is 0.  $W_i^v$  and  $W_j^v$  are the transmit power of VUEi or CUEj on the subcarrier  $v$ .  $\psi_i^v$  and  $\psi_j^v$  are the SINR of VUEi or CUEj on the subcarrier  $v$ , which depends on the channel power gains and the interference from other users.  $\Psi_j^v$  is the data rate of CUEj on the subcarrier  $v$ , which is a function of  $\psi_j^v$ .  $\Psi_j^{size}$  is the minimum data rate requirement size of CUEj, which is a constant value. The objective function is to maximize the sum of the logarithms of  $(1 + \psi_i^v)$  for all VUEs and subcarriers, which is equivalent to maximizing the sum of the data rates of the VUEs. For the constraints,  $c1$  represents that the binary variables  $C_i^v$  and  $C_j^v$  must be either 0 or 1.  $c2$  is that each subcarrier can only be used by one CUE, to avoid interference among CUEs.  $c3$  and  $c4$  are the transmit power of VUEs and CUEs and must not exceed their maximum values, which are  $W_i^{max}$  and  $W_j^{max}$ , respectively.  $c5$  is the sum of the data rates of CUEj on all subcarriers which must be greater than or equal to  $\Psi_j^{size}$ , to ensure the quality of service of CUEs.

### 3. Multiaccess Resource Allocation Algorithms and Power Control

The equation presented above involves binary variables  $\{C_i^v, C_j^v\}$  and a continuous variable. This formulation represents a challenging MINP issue, which poses difficulties in obtaining optimal solutions. Hence, this article undertakes the task of breaking down the MINP problem into two distinct sub-problems. The first issue to be addressed is the multiaccess channel matching problem involving both CUEs and VUEs. Furthermore, there are power control concerns associated with VUEs. A heuristic approach was developed to collectively assign subcarriers for CUEs and VUEs to address the issue of allocating multiaccess resources. Subsequently, the issue about power has been resolved. This work employs a continuous convex technique as a solution to the non-convex optimization problem it addresses. The SCA technique is employed to convert non-convex problems into convex problems, hence enabling their solution. The reason for dividing the initial *Problem 1* into two sub-problems *Problem 2* and *Problem 3* is to simplify the optimization procedure and reduce the computational complexity. The splitting process yields several advantages. Firstly, it reduces the complexity and computational expense of solving the original *Problem 1*, which is inherently difficult. Secondly, it separates the binary and continuous variables, allowing them to be solved independently using distinct methods. Lastly, it achieves a

solution that is nearly optimal, maximizing the sum rate of the VUEs while adhering to the constraints imposed by the CUEs and power limits.

### 3.1. Resource-Allocation Algorithm

In order to effectively utilize limited spectrum resources and better satisfy the demanding data rate needs of VUEs, a multiaccess resource-allocation mechanism is implemented. The allocation technique and interference arising from the shared channel exhibit a higher level of complexity; yet, they have the potential to greatly enhance spectrum usage and data transmission rates. In order to address the subcarrier-allocation issue, this study initially considers binary variables  $\{C_i^v, C_j^v\}$  to be determined as either 0 or 1. It further assumes that the power of CUEs is set to the highest value ( $W_j^{\max} = W_j^v$ ), while the power of VUEs is uniformly distributed among all subcarriers ( $W_i^v = W_i^{\max}/V$ ). Consequently, Problem 1 is restated as

$$\begin{aligned} \text{Problem 2 : } & \max_{\{C_i^v, C_j^v\}} \sum_{i=1}^X \sum_{v=1}^V (\log(1+\psi_i^v)), \\ & \text{s.t.} \\ c1 : & C_i^v, C_j^v \in \{0, 1\}, \forall v \in V, \forall j \in Y, \forall i \in X, \\ c2 : & \sum_j^Y C_j^v \leq 1, \forall v \in V, \\ c5 : & \sum_{v=1}^V \Psi_j^v \geq \Psi_j^{\text{size}}, \forall j \in Y, \end{aligned} \quad (5)$$

Problem 2 includes binary allocation variable constraints and basic data rate requirements for CUEs. The multiaccess heuristic resource-allocation algorithms used in this article are divided into three stages: CUEs' subcarrier allocation, VUEs' subcarrier allocation, and VUEs' multiplexing subcarriers. Figure 2 shows the flowchart of the resource-allocation algorithm. Step 1: To ensure the minimum data rate requirement for CUEs, first we allocate subcarriers to CUEs and maximize the distance data rate requirement ( $j^* = \max(\Delta\Psi_j) = \max(\Psi_j^{\text{size}} - \Psi_j)$ ), allocating the subcarrier  $v^*$  ( $v^* = \max(a_{i^*}^v)$ ) with the highest channel gain to CUE $j^*$ . This step concludes either when all CUEs satisfy the data rate criteria or when all subcarriers have been allocated. If there exist any subcarriers that have not been allocated in the current stage, the system should advance to the second stage. Otherwise, it should go to the third stage. This stage ensures that the CUEs have exclusive access to their assigned subcarriers, and that the orthogonality between subcarriers is maintained. This stage also takes into account the channel quality and the rate demand of each CUE on each subcarrier, which is enabled by OFDMA. Step 2: Allocate the remaining subcarriers to VUEs, and allocate the subcarrier with the best channel gain ( $[v^*, i] = \max a_i^v$ ) to VUEs. This stage ends when all remaining subcarriers are allocated. Step 3: In order to fully utilize spectrum resources, VUEs can reuse subcarriers already allocated to other users.

To determine the optimal VUE for a given subcarrier, it is necessary to identify the unused VUE with the maximum gain on the corresponding channel. The potential for VUE to reuse this subcarrier can be categorized into two distinct scenarios: The subcarrier has been previously allocated a CUE, and it is imperative to determine whether the combined interference resulting from VUE multiplexing will interfere with the fulfillment of the CUE's data rate prerequisites. If this is the case, the practice of multiplexing is prohibited, resulting in the discontinuation of the current subcarrier multiplexing. Contrary to the initial assertion, it is permissible. Subsequently, we proceed to examine the subsequent set of VUEs until the cumulative interference fails to satisfy the data rate prerequisites of the CUE. The process of multiplexing the current subcarrier concludes and transitions to the subsequent subcarrier. The CUE system does not utilize the subcarrier in question, but it is permissible for the VUE system to utilize it in order to transition to the subsequent subcarrier.

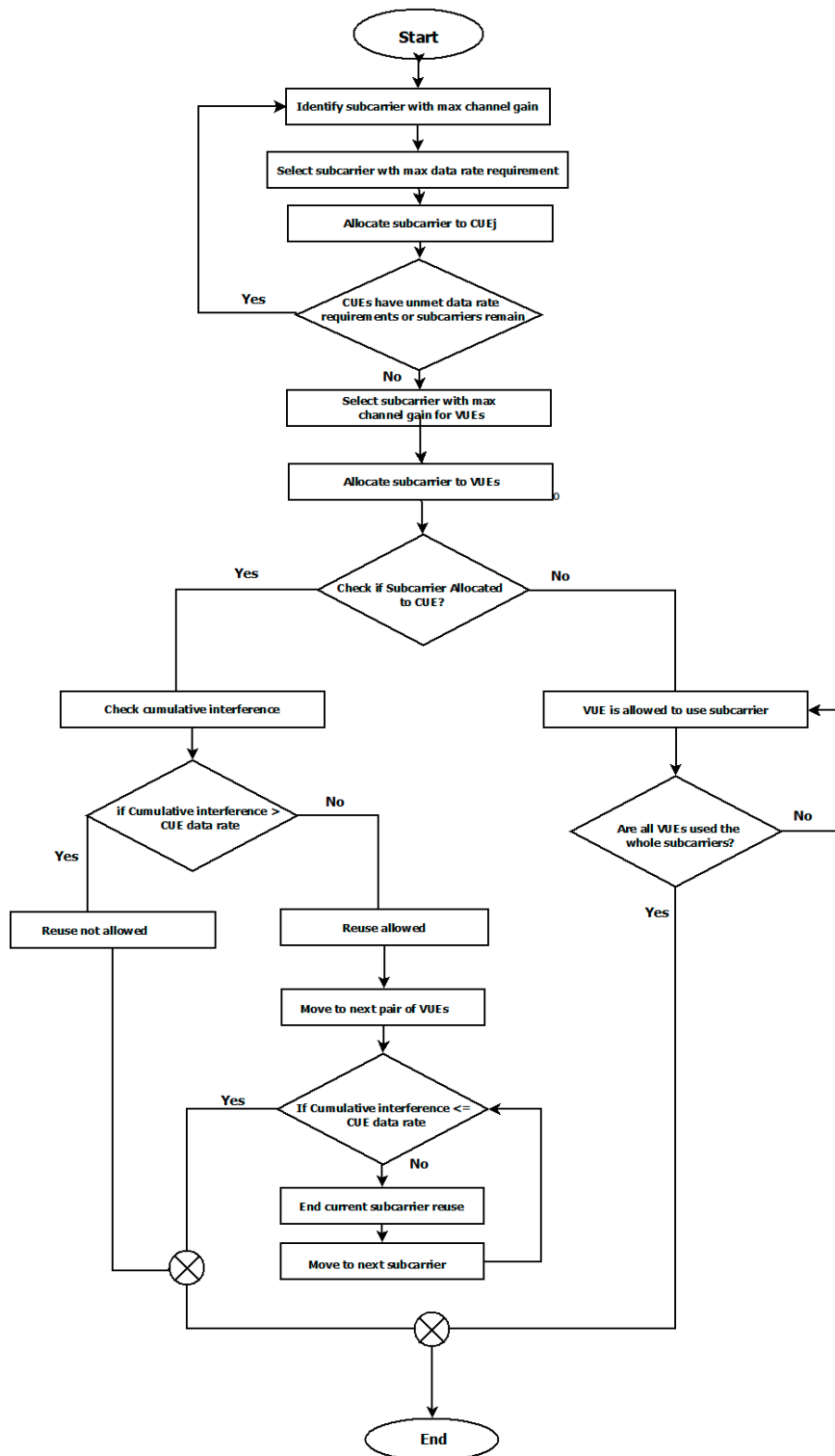


**Figure 2.** Flowchart of the resource-allocation algorithm.

The procedure mentioned above is a resource-allocation algorithm consisting of three stages. Within the algorithm, the assignment of the subcarrier  $v$  to  $VUE_i$  is denoted by the expression  $\text{allocated } VUE(i, v) = 1$ , whereas the assignment of subcarrier  $v$  to  $CUE_j$  is denoted by the expression  $\text{allocated } CUE(j, v) = 1$ . The algorithmic stages are presented in Algorithm 1.

**Algorithm 1:** Pseudocode for multiaccess resource allocation

---

**Input:**  $E_v$ : set of CUEs using subcarrier  $v$ ,  $F$ : set of subcarriers  
 $B_v$ : set of VUEs using subcarrier  $v$   
 $B_{fv}$ : set of VUEs that do not use subcarrier  $v$

**Output:** allocation of resources

1. Begin
2. **Prepare Initialization:**  $W_j^v = W_j^{\max}$ ,  $W_i^v = \frac{W_i^{\max}}{V}$ ,  $\Delta\Psi_j = \Psi_j^{\text{size}} - \Psi_j$
3. **While**  $F$  is not empty or any CUE's data rate requirement is not satisfied **then**
4.   **Select**  $j^* = \max(\Delta\Psi_j)$ , that is, the  $j^*$  th CUE
5.   **Select**  $v^* = \max(a_j^v)$ , that is, allocate the  $v^*$  th subcarrier to the CUE  $j^*$
6.   **Else Recalculate**  $\Psi_j$ ,  $\Delta\Psi_j$ , and remove subcarrier  $v^*$  from set  $F$
7.   **End while**
8.   **When**  $F$  is not empty **do**
9.     Allocate the subcarrier with the best channel gain for VUEs
10.   **End When**
11.   **For** each subcarrier  $v$  **do**
12.     Select the VUE with the largest channel gain ratio in  $B_{fv}$
13.     **If**  $E_v$  is not empty **then**
14.       Calculate the data rate of CUE using subcarrier  $v$
15.       **Else if** the CUE's data rate requirement is still satisfied **then**
16.       **Allow reuse**, check the next subcarrier
17.       **else** the next VUE user until the cumulative interference makes the CUE's data rate requirement unsatisfied, **then**
18.       **Check** the next subcarrier
19.       **End elseif**
20.       **Else**  $E_v$  is empty
21.       **Allow** the VUE to use subcarrier  $v$
22.     **End for end If**
23.   **End**

---

### 3.2. Power-Optimization Algorithms

The utilization of a multiaccess channel matching system in this study enables the possibility of several users sharing a common subcarrier. Consequently, the issue of interference among users inside the same channel becomes significantly complicated. Therefore, in order to alleviate the accumulated interference between users using the same channel, and further improve the throughput of VUEs while ensuring the data rate requirements of CUEs, it is necessary to perform power control. The issue of allocating spectrum resources has been addressed in the preceding section, where the binary variables  $\{C_i^v, C_j^v\}$  were determined. The signal-to-interference-plus-noise ratio (SINR) of VUE  $i$  on the  $v$ -th subcarrier is now being redefined.

$$\psi_i^v = \frac{W_i^v a_i^v}{\theta^2 + \sum_{i' \in B_v, i' \neq i} W_i^v a_{i',i}^v + \sum_{j \in E_v} W_j^v a_{j,i}^v}, \quad (6)$$

The corresponding power control problem is then formulated as

$$\begin{aligned} \text{Problem 3 : } & \max_{\{W_i^v\}} \sum_{i=1}^X \sum_{v=1}^V (\log(1 + \psi_i^v)), \\ & \text{s.t.} \\ & c3 : W_i^v \leq W_i^{\max}, \forall i \in X, \\ & c4 : W_j^v \leq W_j^{\max}, \forall j \in Y, \\ & c5 : \sum_{v=1}^V C_j^v \Psi_j^v \geq \Psi_j^{\text{size}}, \forall j \in Y, \end{aligned} \quad (7)$$

We examine the inherent non-convexity of the optimization problem, which presents significant challenges in its resolution, particularly within the context of multiaccess resource allocation. Since *Problem 3* has a non-convex objective function and the constraint *c5*, *Problem 3* is a non-convex optimization problem, and it is usually difficult to solve in the scenario of multiaccess resource allocation. In order to tackle this issue, we utilize the SCA technique. The fundamental concept underlying SCA involves the conversion of a non-convex problem (*Problem 4*) into a convex problem (*Problem 5*). The problem is solved iteratively using a convex optimization toolbox called CVX [49] until convergence is attained.

By applying the characteristics of logarithmic functions, we can convert the given expression into the conventional D.C form, where  $q(W)$  and  $s(W)$  represent concave functions, as will be demonstrated in *Problem 4*. The process of transformation encompasses the alteration of both the objective function and the constraint *c5*.

First, the objective function transformation

$$q_i(W) - s_i(W), \quad (8)$$

where  $q_i(W)$  and  $s_i(W)$  are, respectively,

$$q_i(W) = \sum_{v=1}^V \log(W_i^v a_i^v + \theta^2 + \sum_{i' \in B_v, i' \neq i} W_i^v a_{i',i}^v + \sum_{j \in E_v} W_j^v a_{j,i}^v), \quad (9)$$

$$s_i(W) = \sum_{v=1}^V \log(\sum_{i' \in B_v, i' \neq i} W_i^v a_{i',i}^v + \sum_{j \in E_v} W_j^v a_{j,i}^v + \theta^2), \quad (10)$$

Second, we construct and update the constrain *c5* with this conversion

$$q_j(W) - s_j(W), \quad (11)$$

where  $q_j(W)$  and  $s_j(W)$  are, respectively,

$$q_j(W) = \sum_{v=1}^V \log(W_j^v a_j^v + \theta^2 + \sum_i^X C_i^v W_i^v a_{i,D}^v), \quad (12)$$

$$s_j(W) = \sum_{v=1}^V \log(\theta^2 + \sum_i^X C_i^v W_i^v a_{i,D}^v), \quad (13)$$

**Problem reformulation:** By inserting Equations (8) and (11) into Equation (7) as a result of the aforementioned transformation, Problem 3 can be restated.

$$\begin{aligned} \text{Problem 4 : } & \max_{\{W_i^v\}} \sum_{i=1}^X q_i(W) - s_i(W), \\ & \text{s.t.} \\ & c3 : W_i^v \leq W_i^{max}, \forall i \in X, \\ & c4 : W_j^v \leq W_j^{max}, \forall j \in Y, \\ & c5 : q_j(W) - s_j(W) \geq \Psi_j^{size}, \forall j \in Y, \end{aligned} \quad (14)$$

Problem 4 can be characterized as a conventional D.C. expression, representing the difference between two concave functions. The absence of a guarantee on the concavity of the overall function prevents the possibility of solving it using a convex optimization toolbox at this point. Hence, additional modification is required. The utilization of a first-order convex approximation enables the transformation of Problem 4 into a convex problem, facilitating its resolution. The gradients of  $s_i(W)$  and  $s_j(W)$  can be represented in the following manner.

$$\nabla s_i(W) = \frac{1}{\theta^2 + \sum_{i' \in B_v} W_{i'}^v a_{i',i}^v + \sum_{j \in E_v} W_j^v a_{j,i}^v} \vec{e}_i \quad (15)$$

$$\nabla s_j(W) = \frac{1}{\theta^2 + \sum_i^X (C_i^v W_i^v a_{i,D}^v)} \vec{e}_j, \quad (16)$$

where  $\vec{e}_i$  is a matrix of  $(X + Y) * V$ , represented as  $\vec{e}_i(i', v) = \frac{a_{i,i}^v}{\ln 2}$ ,  $e_i(j, v) = \frac{a_{j,i}^v}{\ln 2}$ ,  $i' \neq i$ , where  $v$  is the subcarrier assigned to the  $i$ th VUE and  $j$  is the  $j$ th CUE using the the subcarrier  $v$ th; otherwise,  $\vec{e}_i(i' or j, v) = 0$ . Similarly,  $\vec{e}_j = \frac{a_{i,D}^v}{\ln 2}$  is an  $(X + Y) * V$  matrix, defined as  $\vec{e}_j(i, v) = \frac{a_{i,D}^v}{\ln 2}$ , where  $v$  is the subcarrier assigned to the  $j$ th CUE and  $i$  is the VUE using the  $v$ th subcarrier; otherwise,  $\vec{e}_j(i, v) = 0$ .

The utilization of the first-order Taylor expansion is subsequently employed to estimate the values of  $s_i(W)$  and  $s_j(W)$  within their respective tables. This is demonstrated as

$$s_i(W) = s_i(W^t) + \nabla s_i^T(W^t)(W - W^t), \quad (17)$$

$$s_j(W) = s_j(W^t) + \nabla s_j^T(W^t)(W - W^t), \quad (18)$$

After bringing Equations (17) and (18) into Equation (14), Problem 4 can be represented as

$$\text{Problem 5 : } \max_{\{W_i^v\}} \sum_{i=1}^X q_i(W) - s_i(W^t) + \nabla s_i^T(W^t)(W - W^t),$$

s.t

$$c3 : W_i^v \leq W_i^{max}, \forall i \in X,$$

$$c4 : W_j^v \leq W_j^{max}, \forall j \in Y, \quad (19)$$

$$c5 : q_j(W) - s_j(W^t) + \nabla s_j^T(W^t)(W - W^t) \geq \Psi_j^{size}, \forall j \in Y,$$

The aforementioned Problem 5 represents a conventional convex optimization problem that can be effectively resolved using the CVX convex optimization toolbox. The power variable  $W^0$  is initialized, and the variable  $W^t$  is obtained by solving Problem 5 using a convex optimization toolkit. The variable  $W^t$  is then updated iteratively using the algorithm, such that the first-order Taylor expansion provides a continuous approximation of the variables o and u. This allows for the calculation of the system throughput of the variable  $s_i(W)$  and  $s_j(W)$  VUEs after power optimization. The specific details of the power control algorithm are presented in Algorithm 2.

---

**Algorithm 2:** Pseudocode for power optimization

---

1. **Begin**
  2.  $W^0$ : Initial power
  3. **while Initialization:**  $W^0, \epsilon = 10^{-4}$
  4. **If**  $t = 0$ , number of iterations **then**
  5. **Calculate**  $\Psi^0$  by bringing  $W^0$  into the objective function in Equations (17) and (18).
  6. **for**  $t = t + 1$ ,  $W^t = W^*$  **do**
  7. **Solve Problem 5 and obtain**  $W^*$
  8. **End for**
  9. **Else Bring**  $W^t$  **into Equation (14)**
  10. **Calculate** the  $\Psi^t$  of the objective function
  11. **End if**
  12. **Calculate**  $\Delta\Psi = |\Psi^t - \Psi^{t-1}|$
  13. **Until**  $\Delta\Psi \leq \epsilon$
  14. **End for End while**
  15. **End**
-

#### 4. Simulation Results and Analysis

In order to verify the algorithm proposed in this research work, MATLAB2019a simulations were employed. The data presented in each result plot were subjected to statistical analysis, with a minimum of 400 repetitions, in order to obtain averaged values.

This study follows the simulation configuration of the highway scenario outlined in 3GPP TR 37.885. The model presented in this paper represents a single-directional highway consisting of three lanes, each with a width of 4 m. The overall width of the highway is 12 m, and it spans a length of 3000 m. All vehicles exhibit uniform velocity. The distribution of vehicle positions on the road can be modeled by the Poisson distribution, where the average inter-vehicle distance is influenced by the speed of the cars. The BS is situated in a central location with a radius of 500 m. Additionally, there is a distance of 40 m between the university and the adjacent highway. A random selection is made of X pairs of VUEs and N CUEs from the pool of created cars. It is important to note that VUEs are always formed by nearby vehicles. Table 1 displays the primary simulation parameters utilized in the investigation.

**Table 1.** Simulation parameters.

Parameter	Value Size
Channel model	3GPP Highway
Radius size	500 m
Deployment	3 lanes
Antenna height	1.6 m
Carrier frequency	2 GHz
Noise power	-174 dBm
Channel bandwidth	10 MHz
CUEs quantity	3, 5, 7, 9
Vehicle speed	60–110 km/h
Vehicle distribution	Poisson distribution
Shadow standard deviation	8 dB (CUEs), 3 dB (VUEs)
CUEs path loss	$128.1 + 37.6 \log(d [\text{km}])$
VUEs path loss	LOS in WINNER + B1
$W_{\max}^{\text{max}}$	23 dBm
$W_j^{\text{max}}$	23 dBm

##### 4.1. Analysis of Simulation Results

The study of the findings in this section is divided into two parts. The first part is to validate the presence as outlined in this research report. This research evaluates the system in relation to the current literature, specifically focusing on two key aspects: the access rate of VUEs and the throughput. The subsequent section examines the impact of parameter modifications on the system model's throughput for VUEs, as indicated by the graphical representation of the results.

###### 4.1.1. Comparative Analysis of Access Rate and Throughput

A comparative analysis was conducted, referencing [33,50], focusing on access rates pertaining to VUEs. The non-access rate for VUEs is defined as the proportion of instances where the data rate falls below the predetermined target, relative to the total number of VUEs. The findings, depicted in Figure 3, indicate a correlation between the increase in the number of VUEs and a subsequent rise in the non-access rates for all algorithmically-managed VUEs, consequently leading to a decrease in the overall access rate.

In contrast, the observed access rate in this study exceeds that of the comparative literature. In this particular study, it was found that out of the total 60 VUEs, the non-access rate was determined to be 25%. Consequently, this indicates that there were 45 VUEs that were accessible, accounting for 75% of the total VUEs. In comparison, the non-access rates of the references [33,50] are 54% and 44%, respectively, resulting in accessible counts of 28 and 34 VUEs for both references. This implies that 46% and 56% of the VUEs (28 and 34 VUEs) may be accessed correspondingly. Upon analyzing the curve trend depicted in Figure 3, it becomes evident that there is a notable increase in the performance disparity

between the comparative literature and the present study. Although this solution effectively meets the data rate requirements for CUEs and VUEs, it imposes a constraint on the access rate of VUEs. This limitation arises from the allocation of only one subcarrier to each pair of VUEs.

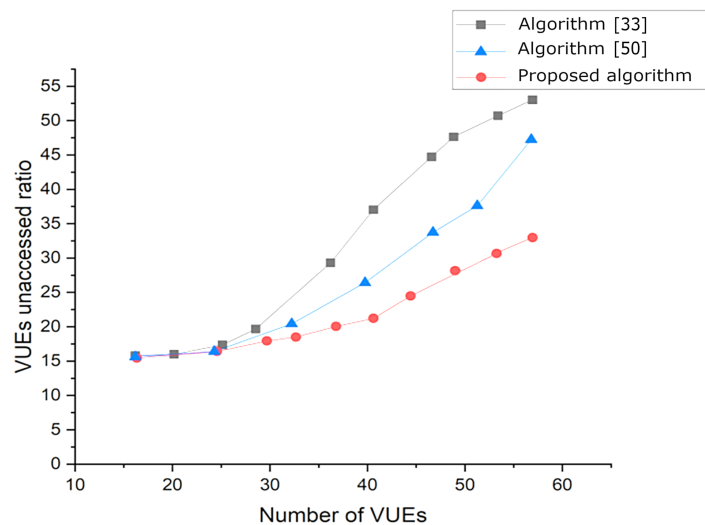


**Figure 3.** Comparison of VUEs' un-access rate.

For the throughput, this study compares throughput using a multiaccess matching method for resource allocation, with references [51,52], where the resource allocation adopts a many-to-one matching scheme; that is, multiple VUEs can use the same subcarrier, and one subcarrier only allows one VUE to use. The random algorithm in [51,52] randomly assigns spectrum resources and power sizes. The comparison, illustrated in Figure 4, indicates a notable enhancement in total VUEs' throughput with the algorithm proposed in this paper. Specifically, when  $\Psi_j^{size} = 5$  for all CUEs, the system data rate of the CUEs hovers around 58.74 (bps/hz) as the number of VUEs increases. In contrast, the data rate of the CUEs in [51,52] gradually decreases with an expanding VUEs count since they do not impose data rate constraints on the CUEs. The proposed algorithm prioritizes meeting CUEs' data rate requirements before resource allocation, employing multiaccess channel matching to fully utilize spectrum resources. Consequently, the total throughput of both VUEs and CUEs systems in this paper surpasses that of the comparative literature. Notably, due to a limited number of subcarriers ( $V = Y = 9$ ), escalating VUEs result in cumulative interference, causing the system throughput to plateau in later stages.

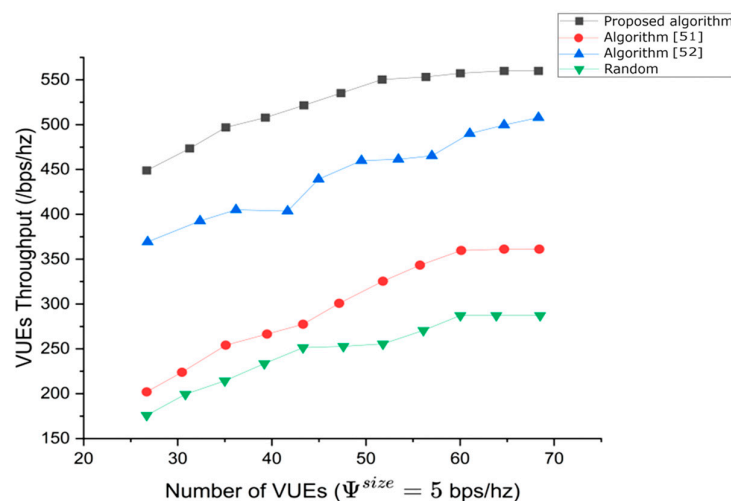


**Figure 4.** Comparison of the VUEs throughput.

#### 4.1.2. Analysis of Model Parameters Change on System Performance

After conducting a thorough review of the relevant literature and establishing the effectiveness of the algorithm presented in this research, we proceed to investigate the influence of changes in system model parameters on the throughput of the VUEs system. This investigation is guided by the outcomes obtained from simulations.

In the first stage, we examine the implications of different quantities of CUEs and their corresponding data rate demands on the throughput of VUEs, as illustrated in Figures 5 and 6, respectively. Significantly, when the number of VUEs increases, there is a corresponding increase in the overall throughput of VUEs. The analysis of Figures 5 and 6 demonstrates a noticeable pattern: when the data rate requirement is consistent, increasing the number of CUEs results in an increase in system throughput. On the other hand, if the quantity of CUEs remains constant while their data rate requirements increase, it leads to a decrease in the system throughput of VUEs. This issue occurs due to the limited number of subcarriers, resulting in a proportional increase in the number of occupied subcarriers by CUEs as their quantity increases.

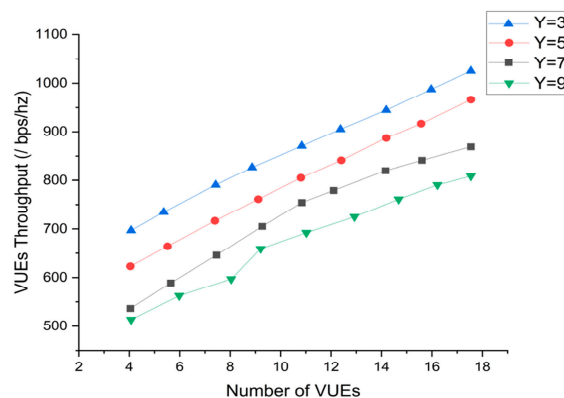


**Figure 5.** Relationship between the CUEs quantity  $Y$  and VUE throughput.

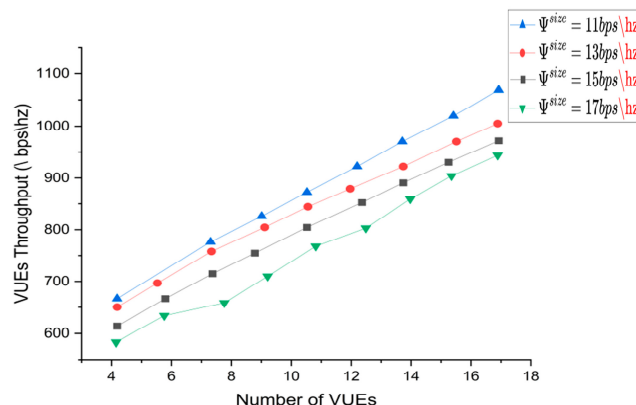


**Figure 6.** Relationship of throughput between  $\Psi^{size}$  (data rate) and VUEs systems.

The increase in data rate requirements for CUEs necessitates a greater utilization of subcarriers in order to meet their data rate demands. Consequently, this leads to an increase in the exhaustion of unassigned subcarriers during the succeeding stage of the resource-allocation process. As a result, the capacity of VUEs to efficiently utilize the spectrum allocated to CUEs decreases, resulting in a decline in the total data transmission rate of VUEs.

Secondly, we will delve into the influence of vehicle speed and the presence or absence of power control on VUEs' throughput, as illustrated in Figure 7. Initially, let us examine the effect of speed. As the vehicle speed escalates, the system throughput of VUEs experiences a decrease, regardless of the presence or absence of power control. This phenomenon arises

from the vehicle position modeling in this study, which considers the vehicle's safe distance. Consequently, the average distance between vehicles increases to ensure driving safety, leading to elevated path loss and subsequently a reduction in VUEs' throughput.

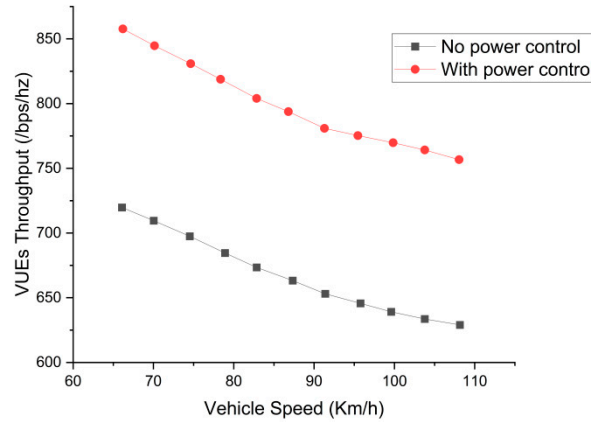


**Figure 7.** Relationship between vehicle speed and VUEs' throughput.

Moving on to the comparison between the presence and absence of power control, the throughput of the system exhibits a higher value with power control in the comparison graph compared to the scenario without power control. This observation underscores the essentiality of power control in this research. The rationale behind this lies in the completion of spectrum resource allocation, wherein binary integer variables are determined. In the absence of power control, VUEs maintain their initial power size, while with power control, VUEs' power size can be automatically adjusted based on spectrum resource allocation without compromising the data rate requirements of CUEs. This adjustment mechanism contributes to an enhancement in the throughput of the VUEs system.

Finally, this study aims to comprehensively analyze the impact of modifying the number of subcarriers on the throughput of VUE systems, as depicted in Figure 8. There is a clear correlation between the increase in the quantity of subcarriers  $V$  and the subsequent rise in the throughput of the VUE system. The origin of this phenomenon can be attributed to the algorithm's increased adaptability in allocating subcarriers to CUEs in the first stage, where the data rate requirements and the number of CUEs remain constant. By increasing the number of subcarriers, the algorithm is able to more efficiently identify the most suitable subcarriers for serving CUEs, which may result in a reduced need for a large number of subcarriers to meet their data rate demands. As a result, during the second stage, a larger set of residual subcarriers is assigned to VUEs, resulting in an overall enhancement of the system throughput for VUEs.

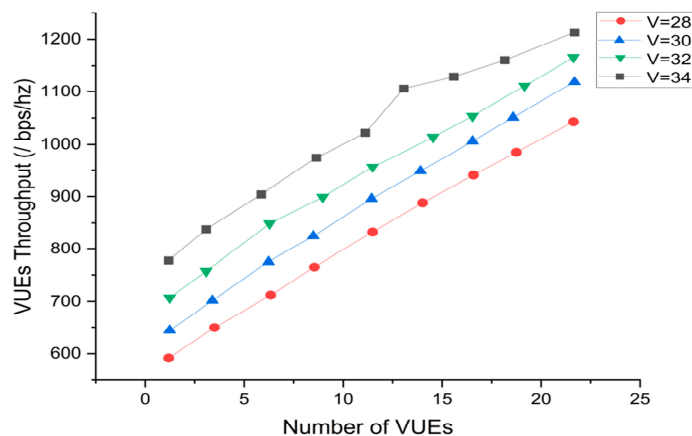


**Figure 8.** The relationship between the number of subcarriers  $V$  and the VUEs throughput.

## 5. Conclusions

In conclusion, the upcoming era of wireless technology holds the potential for a significant and revolutionary influence on V2X communication networks. The pressing issue of scarce spectrum resources, caused by increasing demands for data rates, requires a comprehensive examination of spectrum resource distribution and power regulation. To tackle the intricacy involved in mixed-integer non-linear programming, it is necessary to employ inventive approaches. In order to surmount these obstacles, we utilized a methodical approach, deconstructing the main issue into two separate sub-problems. The resource-allocation difficulty is effectively resolved by implementing a technique for allocating the multiaccess spectrum. This strategy, carefully designed to maximize the utilization of the available spectrum resources, demonstrates a conscious endeavor to improve efficiency. At the same time, the complexities of power regulation are tackled by skillfully applying a technique called continuous convex approximation. This technique transforms difficult non-convex problems into more manageable ones. This two-pronged approach effectively reduces interference between users. The validation process using simulation data clearly and indisputably shows the effectiveness of these approaches in improving vehicle performance. The algorithms presented in this work demonstrate a significant enhancement in system throughput and access rates for VUEs, while simultaneously fulfilling the data rate demands of CUEs. In future works, continuing our research, we recognize the importance of exploring the potential consequences and benefits of cell-free network topologies in the areas of allocating spectrum resources and controlling power for enhancing and optimizing V2X communication systems. The forthcoming studies will involve modifying current algorithms to be compatible with cell-free setups, and thereafter conducting a thorough assessment of their effectiveness in a wide range of different situations. This research provides essential insights and practical answers to the complex field of V2X communication, which will help to develop more reliable and economical connected vehicle systems in the future.

**Author Contributions:** This article was prepared through the collective efforts of all the authors. Conceptualization, A.M.A.I. and Z.C.; methodology, A.M.A.I.; software, A.M.A.I.; validation, A.M.A.I., H.A.E., Y.W. and Z.C.; formal analysis, A.M.A.I. and A.A.I.; investigation, A.M.A.I.; resources, A.M.A.I.; critical review, A.M.A.I., Z.C., H.A.E., Y.W. and A.A.I.; writing—original draft preparation, A.M.A.I.; writing—review and editing, A.M.A.I., Z.C., H.A.E., Y.W. and A.A.I.; supervision, Z.C. All authors have read and agreed to the published version of the manuscript.

**Funding:** This research was funded in part by “the Major Special Project of Changsha Science and Technology Plan under Grant kh2103016” and “the Intelligent software and hardware system of medical process assistant and its application belong to “2030 Innovation Megaprojects”—New Generation Artificial Intelligence under Grant 2020AAA0109605”.

**Institutional Review Board Statement:** Not applicable.

**Informed Consent Statement:** Not applicable.

**Data Availability Statement:** The data presented in this study are available on request from the corresponding author. The data are not publicly available due to restrictions privacy.

**Conflicts of Interest:** The authors declare no conflicts of interest.

## References

1. Ahmed, M.; Mirza, M.A.; Raza, S.; Ahmad, H.; Xu, F.; Khan, W.U.; Lin, Q.; Han, Z. Vehicular Communication Network Enabled CAV Data Offloading: A Review. *IEEE Trans. Intell. Transp. Syst.* **2023**, *24*, 7869–7897. [[CrossRef](#)]
2. Noor-A-Rahim, M.; Liu, Z.; Lee, H.; Khyam, M.O.; He, J.; Pesch, D.; Moessner, K.; Saad, W.; Poor, H.V. 6G for Vehicle-to-Everything (V2X) Communications: Enabling Technologies, Challenges, and Opportunities. *Proc. IEEE* **2022**, *110*, 712–734. [[CrossRef](#)]
3. Shin, C.; Farag, E.; Ryu, H.; Zhou, M.; Kim, Y. Vehicle-to-Everything (V2X) Evolution from 4G to 5G in 3GPP: Focusing on Resource Allocation Aspects. *IEEE Access* **2023**, *11*, 18689–18703. [[CrossRef](#)]
4. Petrov, T.; Pocta, P.; Kovacikova, T. Benchmarking 4G and 5G-Based Cellular-V2X for Vehicle-to-Infrastructure Communication and Urban Scenarios in Cooperative Intelligent Transportation Systems. *Appl. Sci.* **2022**, *12*, 9677. [[CrossRef](#)]

5. Sehla, K.; Nguyen, T.M.T.; Pujolle, G.; Velloso, P.B. Resource Allocation Modes in C-V2X: From LTE-V2X to 5G-V2X. *IEEE Internet Things J.* **2022**, *9*, 8291–8314. [[CrossRef](#)]
6. Raza, S.; Wang, S.; Ahmed, M.; Anwar, M.R.; Mirza, M.A.; Khan, W.U. Task Offloading and Resource Allocation for IoV Using 5G NR-V2X Communication. *IEEE Internet Things J.* **2022**, *9*, 10397–10410. [[CrossRef](#)]
7. Garcia, M.H.C.; Molina-Galan, A.; Boban, M.; Gozalvez, J.; Coll-Perales, B.; Sahin, T.; Kousaridas, A. A Tutorial on 5G NR V2X Communications. *IEEE Commun. Surv. Tutor.* **2021**, *23*, 1972–2026. [[CrossRef](#)]
8. Bazzi, A.; Campolo, C.; Todisco, V.; Bartoletti, S.; Decarli, N.; Molinaro, A.; Berthet, A.O.; Stirling-Gallacher, R.A. Toward 6G Vehicle-to-Everything Sidelink: Nonorthogonal Multiple Access in the Autonomous Mode. *IEEE Veh. Technol. Mag.* **2023**, *18*, 50–59. [[CrossRef](#)]
9. Abdel Hakeem, S.A.; Hussein, H.H.; Kim, H.W. Vision and Research Directions of 6G Technologies and Applications. *J. King Saud Univ.-Comput. Inf. Sci.* **2022**, *34*, 2419–2442. [[CrossRef](#)]
10. Dhinesh Kumar, R.; Rammohan, A. Revolutionizing Intelligent Transportation Systems with Cellular Vehicle-to-Everything (C-V2X) Technology: Current Trends, Use Cases, Emerging Technologies, Standardization Bodies, Industry Analytics and Future Directions. *Veh. Commun.* **2023**, *43*, 100638.
11. Kiela, K.; Barzdenas, V.; Jurgo, M.; Macaitis, V.; Rafanavicius, J.; Vasjanov, A.; Kladovscikov, L.; Navickas, R. Review of V2X-IoT Standards and Frameworks for ITS Applications. *Appl. Sci.* **2020**, *10*, 4314. [[CrossRef](#)]
12. Gyawali, S.; Xu, S.; Qian, Y.; Hu, R.Q. Challenges and Solutions for Cellular Based V2X Communications. *IEEE Commun. Surv. Tutor.* **2020**, *23*, 222–255. [[CrossRef](#)]
13. Zhou, H.; Xu, W.; Chen, J.; Wang, W. Evolutionary V2X Technologies Toward the Internet of Vehicles: Challenges and Opportunities. *Proc. IEEE* **2020**, *108*, 308–323. [[CrossRef](#)]
14. Bahonar, M.H.; Omidi, M.J.; Yanikomeroglu, H. Low-Complexity Resource Allocation for Dense Cellular Vehicle-to-Everything (C-V2X) Communications. *IEEE Open J. Commun. Soc.* **2021**, *2*, 2695–2713. [[CrossRef](#)]
15. Guo, C.; Liang, L.; Li, G.Y. Resource Allocation for Vehicular Communications with Low Latency and High Reliability. *IEEE Trans. Wirel. Commun.* **2019**, *18*, 3887–3902. [[CrossRef](#)]
16. Nguyen, H.T.; Noor-A-Rahim, M.; Guan, Y.L.; Pesch, D. Cellular V2X Communications in the Presence of Big Vehicle Shadowing: Performance Analysis and Mitigation. *IEEE Trans. Veh. Technol.* **2023**, *72*, 3764–3776. [[CrossRef](#)]
17. Chen, S.; Hu, J.; Zhao, L.; Zhao, R.; Fang, J.; Shi, Y.; Xu, H. *Wireless Networks Cellular Vehicle-to-Everything (C-V2X)*; Springer Nature: Berlin/Heidelberg, Germany, 2023.
18. Jiang, W.; Han, B.; Habibi, M.A.; Schotten, H.D. The Road towards 6G: A Comprehensive Survey. *IEEE Open J. Commun. Soc.* **2021**, *2*, 334–366. [[CrossRef](#)]
19. Liu, Q.; Liang, H.; Luo, R.; Liu, Q. Energy-Efficiency Computation Offloading Strategy in UAV Aided V2X Network with Integrated Sensing and Communication. *IEEE Open J. Commun. Soc.* **2022**, *3*, 1337–1346. [[CrossRef](#)]
20. Murroni, M.; Anedda, M.; Fadda, M.; Ruiu, P.; Popescu, V.; Zaharia, C.; Giusto, D. 6G—Enabling the New Smart City: A Survey. *Sensors* **2023**, *23*, 7528. [[CrossRef](#)]
21. Brahmi, I.; Koubaa, H.; Zarai, F. Resource Allocation for Vehicle-to-Everything Communications: A Survey. *IET Netw.* **2023**, *12*, 98–121. [[CrossRef](#)]
22. He, X.; Yang, X.; Lv, J.; Zhao, J.; Luo, T.; Chen, S. A Cluster-Based UE-Scheduling Scheme for NR-V2X. *IEEE Trans. Veh. Technol.* **2023**, *72*, 4538–4552. [[CrossRef](#)]
23. Arikumar, K.S.; Prathiba, S.B.; Basheer, S.; Moorthy, R.S.; Dumka, A.; Rashid, M. V2X-Based Highly Reliable Warning System for Emergency Vehicles. *Appl. Sci.* **2023**, *13*, 1950. [[CrossRef](#)]
24. Li, Z.; Wang, S.; Zhang, S.; Wen, M.; Ye, K.; Wu, Y.C.; Ng, D.W.K. Edge-Assisted V2X Motion Planning and Power Control Under Channel Uncertainty. *IEEE Trans. Veh. Technol.* **2023**, *72*, 9641–9646. [[CrossRef](#)]
25. Chen, K.L.; Chen, W.Y.; Hwang, R.H. Optimizing Resource Allocation with High-Reliability Constraint for Multicasting Automotive Messages in 5G NR C-V2X Networks. *IEEE Trans. Veh. Technol.* **2023**, *72*, 4792–4804. [[CrossRef](#)]
26. Ngene, C.E.; Thakur, P.; Singh, G. Power Allocation Strategies for 6G Communication in VL-NOMA Systems: An Overview. *Smart Sci.* **2023**, *11*, 475–518. [[CrossRef](#)]
27. Cao, L.; Roy, S.; Yin, H. Resource Allocation in 5G Platoon Communication: Modeling, Analysis and Optimization. *IEEE Trans. Veh. Technol.* **2023**, *72*, 5035–5048. [[CrossRef](#)]
28. Zhao, B.; Liu, J.; Mao, B.; Li, S. Optimal Resource Allocation for Random Multiple Access Oriented SCMA-V2X Networks. *IEEE Trans. Veh. Technol.* **2023**, *72*, 10921–10932. [[CrossRef](#)]
29. Li, R.; Hong, P.; Xue, K.; Zhang, M.; Yang, T. Energy-Efficient Resource Allocation for High-Rate Underlay D2D Communications with Statistical CSI: A One-to-Many Strategy. *IEEE Trans. Veh. Technol.* **2020**, *69*, 4006–4018. [[CrossRef](#)]
30. He, C.; Chen, Q.; Pan, C.; Li, X.; Zheng, F.C. Resource Allocation Schemes Based on Coalition Games for Vehicular Communications. *IEEE Commun. Lett.* **2019**, *23*, 2340–2343. [[CrossRef](#)]
31. Liu, Y.; Wang, W.; Chen, H.H.; Wang, L.; Cheng, N.; Meng, W.; Shen, X. Secrecy Rate Maximization via Radio Resource Allocation in Cellular Underlaying V2V Communications. *IEEE Trans. Veh. Technol.* **2020**, *69*, 7281–7294. [[CrossRef](#)]
32. Afifi, W.S.; El-Moursy, A.A.; Saad, M.; Nassar, S.M.; El-Hennawy, H.M. A Novel Scheduling Technique for Improving Cell-Edge Performance in 4G/5G Systems. *Ain Shams Eng. J.* **2021**, *12*, 487–495. [[CrossRef](#)]

33. Aslani, R.; Saberinia, E.; Rasti, M. Resource Allocation for Cellular V2X Networks Mode-3 with Underlay Approach in LTE-V Standard. *IEEE Trans. Veh. Technol.* **2020**, *69*, 8601–8612. [[CrossRef](#)]
34. Jameel, F.; Khan, W.U.; Kumar, N.; Jantti, R. Efficient Power-Splitting and Resource Allocation for Cellular V2X Communications. *IEEE Trans. Intell. Transp. Syst.* **2021**, *22*, 3547–3556. [[CrossRef](#)]
35. Zhang, E.; Yin, S.; Ma, H. Stackelberg Game-Based Power Allocation for V2X Communications. *Sensors* **2020**, *20*, 58. [[CrossRef](#)] [[PubMed](#)]
36. Ghosh, J.; Gupta, A.; Haci, H.; Jakó, Z. User Association, Power Control and Channel Access Schemes for Two-Tier Macro-Femto Networks: CDF of SINR Analysis. *IETE Tech. Rev. (Inst. Electron. Telecommun. Eng. India)* **2022**, *39*, 219–230. [[CrossRef](#)]
37. Liang, L.; Li, G.Y.; Xu, W. Resource Allocation for D2D-Enabled Vehicular Communications. *IEEE Trans. Commun.* **2017**, *65*, 3186–3197. [[CrossRef](#)]
38. Chen, Y.; Wang, Y.; Zhang, J.; Renzo, M. Di QoS-Driven Spectrum Sharing for Reconfigurable Intelligent Surfaces (RISs) Aided Vehicular Networks. *IEEE Trans. Wirel. Commun.* **2021**, *20*, 5969–5985. [[CrossRef](#)]
39. Liang, L.; Xie, S.; Li, G.Y.; Ding, Z.; Yu, X. Graph-Based Resource Sharing in Vehicular Communication. *IEEE Trans. Wirel. Commun.* **2018**, *17*, 4579–4592. [[CrossRef](#)]
40. Wang, P.; Wu, W.; Liu, J.; Chai, G.; Feng, L. Joint Spectrum and Power Allocation for V2X Communications with Imperfect CSI. *arXiv* **2023**, arXiv:2302.14704. [[CrossRef](#)]
41. Xiao, H.; Zhu, D.; Chronopoulos, A.T. Power Allocation with Energy Efficiency Optimization in Cellular D2D-Based V2X Communication Network. *IEEE Trans. Intell. Transp. Syst.* **2020**, *21*, 4947–4957. [[CrossRef](#)]
42. Guo, C.; Liang, L.; Li, G.Y. Resource Allocation for Low-Latency Vehicular Communications: An Effective Capacity Perspective. *IEEE J. Sel. Areas Commun.* **2019**, *37*, 905–917. [[CrossRef](#)]
43. Li, X.; Ma, L.; Xu, Y.; Shankaran, R. Resource Allocation for D2D-Based V2X Communication with Imperfect CSI. *IEEE Internet Things J.* **2020**, *7*, 3545–3558. [[CrossRef](#)]
44. Liu, Z.; Xie, Y.; Chan, K.Y.; Ma, K.; Guan, X. Chance-Constrained Optimization in D2D-Based Vehicular Communication Network. *IEEE Trans. Veh. Technol.* **2019**, *68*, 5045–5058. [[CrossRef](#)]
45. Thakur, P.; Singh, G. *Spectrum Sharing in Cognitive Radio. Networks Towards Highly Connected Environments*; John Wiley & Sons: Hoboken, NJ, USA, 2021; ISBN 9781119665427.
46. Ali, Z.; Lagen, S.; Giupponi, L.; Rouil, R. 3GPP NR V2X Mode 2: Overview, Models and System-Level Evaluation. *IEEE Access* **2021**, *9*, 89554–89579. [[CrossRef](#)] [[PubMed](#)]
47. Ming, Y.; Chen, J.; Dong, Y.; Wang, Z. Evolutionary Game Based Strategy Selection for Hybrid V2V Communications. *IEEE Trans. Veh. Technol.* **2022**, *71*, 2128–2133. [[CrossRef](#)]
48. Guo, C.; Wang, C.; Cui, L.; Zhou, Q.; Li, J. Radio Resource Management for C-V2X: From a Hybrid Centralized-Distributed Scheme to a Distributed Scheme. *IEEE J. Sel. Areas Commun.* **2023**, *41*, 1023–1034. [[CrossRef](#)]
49. Liu, A.; Lau, V.K.N.; Kanarian, B. Stochastic Successive Convex Approximation for Non-Convex Constrained Stochastic Optimization. *IEEE Trans. Signal Process.* **2019**, *67*, 4189–4203. [[CrossRef](#)]
50. Thakur, K.P.; Palit, B. A QoS-Aware Joint Uplink Spectrum and Power Allocation with Link Adaptation for Vehicular Communications in 5G Networks. *arXiv* **2023**, arXiv:2305.02667.
51. Gyawali, S.; Qian, Y.; Hu, R.Q. Resource Allocation in Vehicular Communications Using Graph and Deep Reinforcement Learning. In Proceedings of the 2019 IEEE Global Communications Conference (GLOBECOM), Waikoloa, HI, USA, 27 February 2019; pp. 1–6.
52. Parizi, M.I.; Pourmoslemi, A.; Rajabi, S.; Cumanan, K. Power Control and Fuzzy Pairing in V2X Communications. *IEEE Syst. J.* **2023**, *17*, 2390–2398. [[CrossRef](#)]

**Disclaimer/Publisher’s Note:** The statements, opinions and data contained in all publications are solely those of the individual author(s) and contributor(s) and not of MDPI and/or the editor(s). MDPI and/or the editor(s) disclaim responsibility for any injury to people or property resulting from any ideas, methods, instructions or products referred to in the content.